 doi:10.20944/preprints202001.0195.v1

Immune Landscape in Burkitt Lymphoma reveals M2-macrophage polarization and Correlation between PD-L1 expression and Non-Canonical EBV latency program

Massimo Granai[§£]*, Lucia Mundo[£]*, Ayse U Akarca[^], Maria Chiara Siciliano [£], Hasan Rizvi[^^], Ester Sorrentino, Virginia Mancini[£], Maha Ibrahim[˙], Sandra Margielewska″, Wenbin Wei″, Michele Bibas[·], Noel Onyango[˜], Joshua Nyagol[˜], Pier Paolo Piccaluga[°°], Leticia Quintanilla- Martinez[§], Falko Fend[§], Stefano Lazzi[£], Lorenzo Leoncini[£], Teresa Marafioti[°^]

*Equally contributed

£ Department of Medical Biotechnology, University of Siena, Siena, Italy.

§ University Hospital of Tübingen, Institute of Pathology, Tübingen, Germany

^ Department of Pathology, University College London, London UK

° Department of Cellular Pathology, University College Hospital, London, London UK

^^Department of Cellular Pathology, Barts Health NHS Trust, London, UK

~ Department of Human Pathology, University of Nairobi, Kenya

″Institute of Immunology and Immunotherapy, University of Birmingham, Birmingham, UK

˙South Egypt Cancer Institute, Assiut University, Assiut, Egypt

·Clinical Department, National Institute for Infectious Diseases "Lazzaro Spallanzani" I.R.C.C.S., Rome, Italy

°° Department of Experimental, Diagnostic, and Specialty Medicine Bologna University Medical School, S. Orsola Malpighi Hospital, Bologna; Euro-Mediterranean Institute of Science and Technology (IEMEST), Palermo, Italy and Department of Pathology, Jomo Kenyatta University of Agriculture and technology, Nairobi, Kenya;

 doi:10.20944/preprints202001.0195.v1

Abstract

The Tumor Microenviroment (TME) is a complex milieu that is increasingly recognized as a key factor in multiple stages of disease progression and responses to therapy as well as escape from immune surveillance. However, the precise contribution of specific immune effector and immune suppressor components of the TME in Burkitt lymphoma (BL) remains poorly understood. In this paper, we applied the computational algorithm CIBERSORT to Gene Expression Profile (GEP) datasets of 40 BL samples to draw a map of immune and stromal components of TME. Furthermore, by VECTRA multispectral immunofluorescence (IF) and multiple immunohistochemistry (IHC), we investigated the TME of an additional series of 40 BL cases and evaluated the possible role of the PD-1/PD-L1 immune checkpoint axis. Our results indicated that M2 polarized macrophages are the most prominent TME component in BL. In addition, we investigated the correlation between PD-L1 and latent membrane protein-2A (LMP2A) expression on tumour cells, highlighting a subgroup of BL cases characterized by a non- canonical latency program of EBV with an activated PD-L1 pathway. In conclusion, our study analysed the TME in BL and identified a tolerogenic immune signature highlighting new potential therapeutic targets.

Preprints (www.preprints.org) | NOT PEER-REVIEWED | Posted: 18 January 2020 doi:10.20944/preprints202001.0195.v1

Introduction

Over recent years, the understanding of the biology of B-cell lymphoma has advanced significantly with the identification of the role played by the tumour microenvironment (TME) in lymphomagenesis[1,2]. The TME of B-cell lymphomas mainly contains variable numbers of mesenchymal stem cells, immune cells and soluble factors. The complex interplay between tumour cells and TME regulates tumorigenesis and provides novel targets for immunotherapies [3,4]. In aggressive lymphomas, particularly in BL, due to their high proliferation rate, intensive chemotherapy is required to counteract proliferation and dissemination of neoplastic cells. Unfortunately, these burdensome treatments are not as effective in elderly and immunocompromised patients [5]. Furthermore, in equatorial Africa, where BL is the most common childhood cancer, the prognosis of BL is still poor because intensive therapeutic regimens would be too toxic for use in African setting[6-10]. Shortcomings of current BL therapies make the exploration of new therapeutic avenues a substantial and reasonable aim [7]. Therefore, a proper characterization of the TME in BL might be helpful to identify alternative therapeutic targets.

One of the histological hallmarks of BL is the high content of tumour-associated macrophages (TAMs) involved in apoptotic tumour cell clearance that confer the so-called starry-sky appearance being [11]. Although little is known about the functional status of macrophages and their impact on tumour immune response in BL, TAMs may function as potential mediator of tumour progression through secretion of chemokines, cytokines and expression of immune checkpoint- associated proteins as programmed- death- ligand 1 (PD-L1). [12,13]

The expression of PD-L1 in B-cell lymphoma remains controversial, especially in BL. Indeed, PD-L1 has been reported in 80% of BL cases (8 out 10) by Majzner[14]. However, this result was not reproduced by others[15]. Moreover, the role of the antigenic signature of Epstein Barr virus (EBV) in modulating the tumour microenvironment and the expression of immune- tolerant proteins has not been analysed in any of these studies. These different and somehow discordant results may be due to the diverse latency program of EBV infected cells and thus to different patterns of viral genes expression.

The constitutive association between EBV and BL, especially with endemic Burkitt lymphoma (eBL) rises questions regarding the role of the virus in altering and actively shaping the tumour microenvironment[16-21]. Indeed, EBV orchestrates a variety of complex mechanism favouring the escape of lymphoma cells from anti-tumour immune responses while promoting the creation of niches in which tumour cells may find support for their growth and survival [19-23].

Preprints (www.preprints.org) | NOT PEER-REVIEWED | Posted: 18 January 2020 doi:10.20944/preprints202001.0195.v1

Computational methods of gene expression profile (GEP) deconvolution allow high sensitivity discrimination of cell subsets within complex tissues, as tumours [24]. These approaches provide quantitative/ functional information also on rare tumour- infiltrating elements, offering the unprecedented opportunity of reanalysing available genomic data to explore TME cells. Here, we applied the computational algorithm CIBERSORT to GEP datasets of 40 BL samples previously published by our group[26], including eBL, sporadic BL (sBL) and idBL cases, to draw a map of immune and stromal components of TME. Finally, to validate GEP preliminary data, we applied multiplex immunohistochemistry to an additional cohort of 24 cases and we further supported these results by performing Vectra analysis on additional 16 BL by immunofluorescence using different antibodies. Thus, a total of 80 BL cases were analysed.

In addition, we investigated the programmed cell death protein -1 (PD-1)/PD-L1 pathway activation status and the possible contribution of EBV in PD-L1 induction as alternative mechanism responsible for the immune evasion.

Material and Methods

CIBERSORT and Gene set enrichment analyses

A CIBERSORT-based deconvolution of GEP datasets (GSE26673) from 40 BL samples (13 eBLs, 21 sBLs 6 idBLs), previously published[26], was carried out using a 547-gene signature matrix customized for characterizing tissue sample immune cell composition, according to CIBERSORT instructions (https://cibersort.stanford.edu/) [25]. EBV status and the viral protein expression in these cases is reported in Table 1. Briefly, normalized gene expression data were used to infer the relative proportions of 22 types of infiltrating immune cells while gene expression datasets were prepared using standard annotation files and data uploaded to the CIBERSORT web portal (http://cibersort.stanford.edu/), with the algorithm run using the default signature matrix at 1000 permutations. Gene set enrichment analysis (GSEA) was run on the same panel of cases (GSE26673), as previously described[25].

Preprints (www.preprints.org) | NOT PEER-REVIEWED | Posted: 18 January 2020 doi:10.20944/preprints202001.0195.v1

		EBNA1+	EBNA1+/LMP1+	EBNA1+/LMP2A+	EBNA1+/LMP1+/LMP2A+	EBV-	Total
Discovery cohort	**eBL**	13	np	np	np	-	13
	sBL	6	np	np	np	15	21
	idBL	5	np	np	np	1	6
Validation cohort 1 (mIF)	**eBL**	11	1	4	-	-	16
	sBL	-	-	-	-	-	-
	idBL	-	-	-	-	-	-
Validation cohort 2 (mIHC)	**eBL**	10	-	2	-	-	12
	sBL	2	-	-	-	6	8
	idBL	4	-	-	-	-	4
		51	1	6	-	22	80

* **np:** not performed

Table 1. EBV status and the viral protein expression of the examined series

Multiplex immunofluorescence staining

Multiplex immunofluorescence (mIF) was carried out on 16 formalin fixed paraffin embedded (FFPE) BL cases (validation cohort 1), belonging to set of samples previously studied and well characterized for EBV latency program[27]. In particular, 11 out of 16 cases showed an EBV latency of type I, while the remaining 5 cases exhibited a non-canonical EBV latency characterized by LMP1 expression in 1 case and LMP2A in the other 4 (Table 1).

Multiplex IF was applied to simultaneously detect the expression of: a) CD68 (Abcam, ab 955, 1:150) and CD163 (Leica Biosystem, 10D6, 1:200); b) PD-L1 (Dako, clone 22C3, 1:100) and CD163 (Leica Biosystem, 10D6, 1:200); c) PD-L1 and EBV-LMP2A (Abcam, clone 15F9, ab59028, 1:200). These double stainings use red and green or magenta and green chromogens. The colour assignment and staining location are: a) CD68 red/membranous; CD163 green/membranous; b) PD-L1, green/membranous and CD163, pink/membranous or PD-L1, green/membranous and CD163, red/membranous; c) PD-L1, red; LMP2A green/ membranous. The staining procedure was established according to previously published work [28]. Briefly, the slides were treated with citrate antigen retrieval buffer and then incubated with the primary (4°C, over night) and secondary (room temperature, 2 hours) antibodies. Tissue sections from the same set of cases and without antibody/fluorophore were used as negative control. Multiplex IF staining reaction and image analysis (including quantification of antibodies expression) were performed using the Vectra 2.0 system (PerkinElmer, Waltham, MA) and TissueFAXSFluo slide scanning system (TissueGnostics, Vienna Austria) based on a Zeiss Axio Imager Z2 upright epifluorescence microscope.

Preprints (www.preprints.org) | NOT PEER-REVIEWED | Posted: 18 January 2020 doi:10.20944/preprints202001.0195.v1

Multiplex immunohistochemistry

An additional validation set (validation cohort 2) of 24 FFPE BL cases (8 sporadic, 12 endemic and 4 HIV-associated) were retrieved from the Departments of Histopathology, University College Hospital, London (UK); Medical Biotechnologies, University of Siena, Siena (Italy); Pathology, University of Nairobi, Kenya and Histopathology and Istituto Lazzaro Spallanzani, Rome (Italy). The diagnosis of BL was issued by expert hematopathologists following the criteria described of the 4th edition of World Health Organization classification of tumours of Haematopoietic and Lymphoid Tissue [29]. Single immunohistochemistry for the diagnostic antibodies and for EBV antigens was carried out on the Bond III Autostainer (Leica, Microsystems, Newcastle upon Tyne, UK) by following the manufacturer's instructions. All of the eBL cases were EBV positive, 10 of which expressed only EBNA1 by IHC while the remaining two were characterized by a non-canonical latency of EBV with the expression of LMP2A. Only two of the 8 sBL cases were EBV positive showing a latency I expression pattern with the sole positivity of EBNA1. All of the idBL cases (4/4) were EBV positive and showed a latency of type I (Table1).

By applying multiplex immunohistochemistry (mIHC), we investigated the simultaneous expression of: a) PD-L1 (ab238697, Abcam, 1:100) in brown, CD-163 (Abcam, Ab87099, 1:100) in red and MYC (Abcam, Ab32072, Y69 clone, 1:150) in blue; b) PD-L1(Abcam, ab238697, 1:100) in brown, CD68 (Abcam, ab 955, 1:150) in red and C-Maf (Abcam, Ab243901, 1:150,) in blue; c) PD-1 (Abcam, NAT105, 1:100) in brown, CD8 (Leica Biosystem,4B1, 1:200) in red and Granzyme B (Abcam134933,marker for T- cell activation) blue. The triple immunostaining was assessed as previously described in Marafioti et al, 2010[30]. These multiple staining use pink, brown and blue chromogens. The colour assignment and staining location are: a) PD-L1 brown/membranous; CD-163 red/membranous; C-MYC blue/nuclear b) PD-L1, brown/membranous; CD163 red/membranous; C-Maf blue/nuclear; c) PD-1 brown/membranous; CD8 red/membranous and Granzyme B blue/nuclear. Tissue sections from the same set of cases and without antibody/chromogens were used as negative control.

The percentage of each cell population characterized by multiplex analysis was then calculated by counting the respective cells in 10 hpf (40x).

Preprints (www.preprints.org) | NOT PEER-REVIEWED | Posted: 18 January 2020 doi:10.20944/preprints202001.0195.v1

RESULTS

CIBERSORT identifies M2- polarized macrophages as the most representative TME component in BL.

The computational algorithm CIBERSORT to GEP datasets from BL samples revealed a heterogeneous reactive milieu with slight differences in tumour microenvironment among the three BL subtypes (endemic, sporadic and HIV-associated), most likely reflecting their underlying immunological status. The analysis showed that macrophages with a M2 profile were the most represented population with CD8-positive T-lymphocyte and CD4 follicular T-helper cells. In contrast, regulatory T-cells and M1 macrophages were poorly represented (Figure 1A-B).

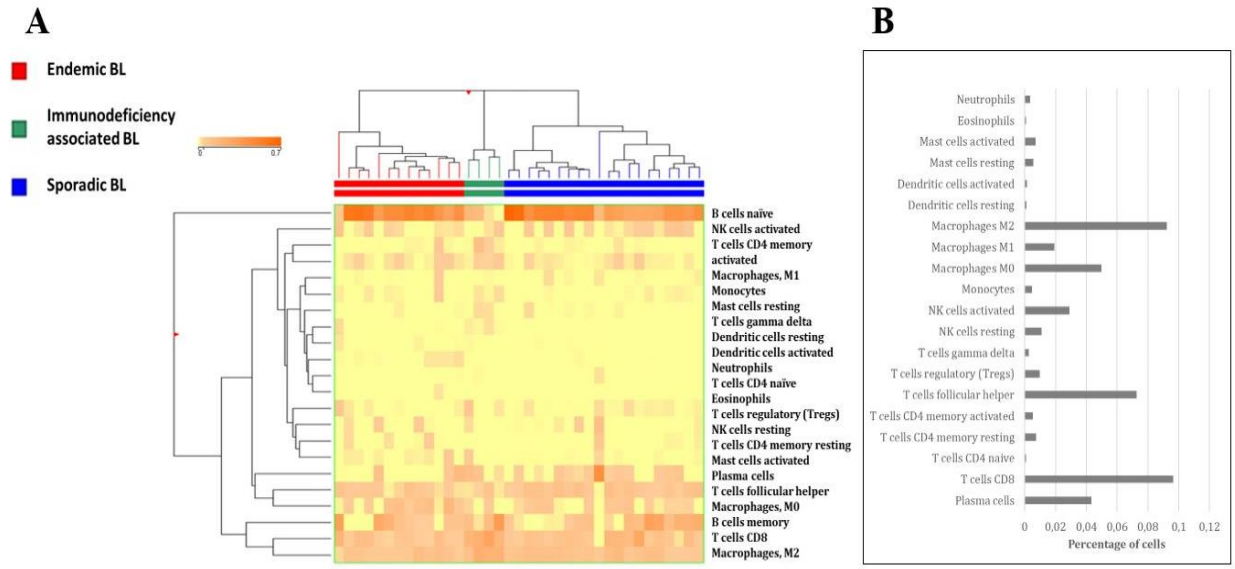

Figure 1. A) Hierarchical clustering of Burkitt lymphoma cases bases on TAM, assessed by CIBERSORT deconvolution. **B)** Immune components in the microenvironment of Burkitt lymphoma cases based on CIBERSORT deconvolution after exclusion of B-cell signature as being referred to the neoplastic components.

Multiplex immunofluorescence confirmed the prevalence of M2 macrophages and revealed a heterogeneous PD-L1 expression.

Tissue samples were studied by mIF and analysed by VECTRA to quantify macrophages and PD-L1 expression on 16 BL samples (validation cohort 1) stained for PD-L1, CD68 and CD163.

In all the cases the M2 macrophages were the most represented population ranging from 66% to 78% of total TAMs (Figure 2), thus confirming the CIBERSORT results. In addition, the vast majority of

Preprints (www.preprints.org) | NOT PEER-REVIEWED | Posted: 18 January 2020 doi:10.20944/preprints202001.0195.v1

them were positive for PD-L1 with a range of expression from 35% to 70% of total macrophages (Figure 3 A-C; Table 2).

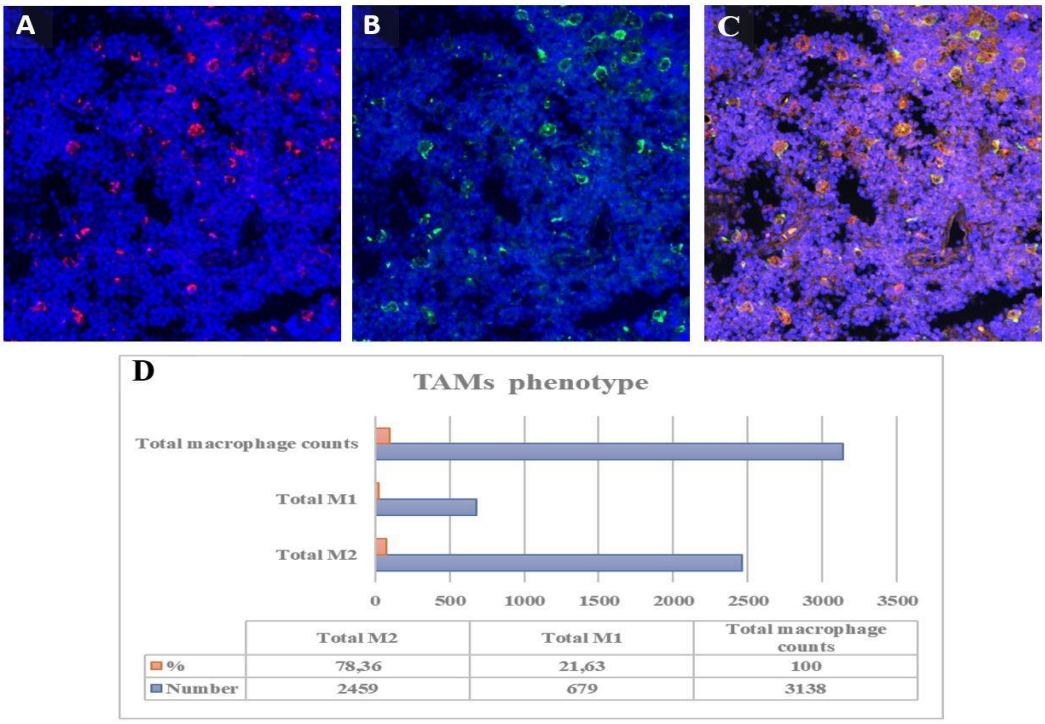

Figure 2. Immunofluorescence staining for Tumor-associated Macrophage Polarization in BL. CD68 (red, A) and CD163 (green, B). Nuclei were stained with DAPI. C shows merge of A,B pictures. D) Example of total macrophages counted by Vectra analysis in one BL case.

Table 2. mIF and VECTRA analysis of macrophages and PD-L1 expression on 16 BL samples (valid. ation cohort 1) stained for PD-L1, CD68 and CD163.

mIF	
Macrophage polarization and PD-L1 expression	**n**
M1	**22-34%**
M2	**66-78%**
n (%) PDL1 (+) CD163(+)	**35-70%**

Preprints (www.preprints.org) | NOT PEER-REVIEWED | Posted: 18 January 2020 doi:10.20944/preprints202001.0195.v1

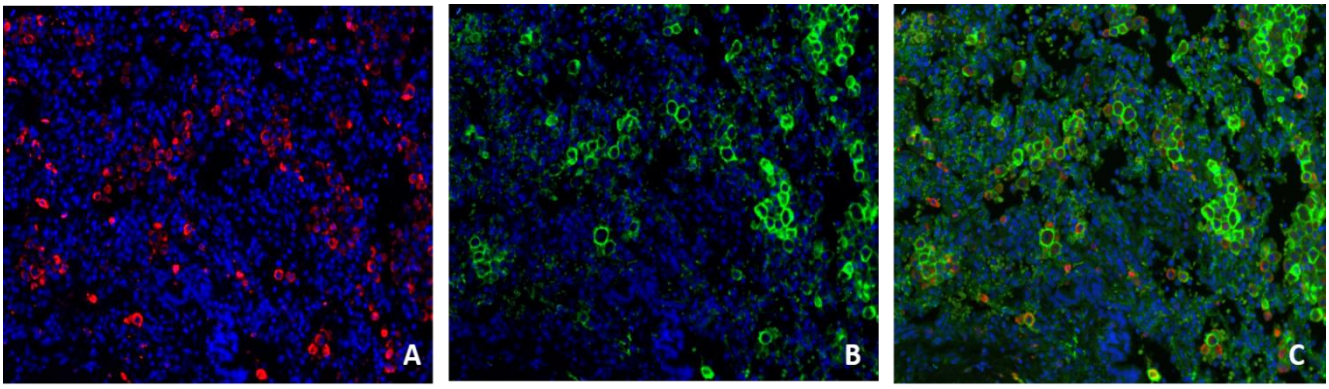

Figure 3. Immunofluorescence staining for PD-L1 and TAMs. The vast majority of M2 TAMs expressed PD-L1. CD163 in red (A), PD-L1 in green (B) and merge (C).

Multiplex IHC showed M2 macrophage polarization, cytotoxic T cells exhaustion and PD-L1 expression in Burkitt lymphoma.

PD-L1 expression and TME were also investigated by mIHC on 24 additional BL samples (validation cohort 2). The analysis confirmed a M1-M2 macrophage ratio shifted towards M2 phenotype ($CD68^+$/ $CD163^+$/$c\text{-}maf^+$) in all BL cases (Table 3, Figure 4A). In particular, the evaluation of M1 macrophages, defined by $CD68^+$, c-maf and CD163 negative cells, showed very similar values among the series ranging from 20 % to 40% of total TAMs. On the other hand, all cases were characterized by a clear prominence of M2 macrophages ($CD68^+$/ $CD163^+$/ c-maf $^+$) ranging from 60% to 80%. PD-L1 expression on TAMs showed similar values for eBL and idBL cases ranging from 65% to 80% and from 55% to 75% respectively. Interestingly, PD-L1 expression on TAMs in sBL showed lower values with a range from 20% to 40%. CD8/ PD-1/ Granzyme B staining highlighted that the vast majority of $CD8^+$ T cells co-expressed PD-1 ranging from 60 to 80% and 50% to 70% of total tumor infiltrating cytotoxic T cells for eBL and idBL respectively (inset Figure 4A). Interestingly, sBL cases, in which EBV was negative to a greater extent (6 out of 8 cases) showed a markedly lower PD-1 expression on CD8 positive T cells ranging from 35% to 50%. These findings suggest a possible correlation between PD-1 induction on tumor infiltrating cytotoxic T-cells and EBV infection.

Preprints (www.preprints.org) | NOT PEER-REVIEWED | Posted: 18 January 2020 doi:10.20944/preprints202001.0195.v1

mIHC for PD-1/PD-L1 expression and macrophage polarization				
		eBL (n=12)	**sBL (n=8)**	**iBL (n=4)**
TAM	M1 (CD68+/c-maf-/CD163-) M2 (CD68+/c-maf+/CD163+)	20-40% 60-80%	30-40% 60-70%	20-30% 70-80%
PD-L1	TAMs (PD-L1+/CD163+)	65-80%	20-40%	55-75%
Exhausted cytotoxic T cells	CD8+/PD1+/Granzyme B-	60-80%	20-40%	60-80%

Table 3. mIHC for macrophages and PD-L1 expression on 24 BL samples (validation cohort 2) stained for PD-L1, CD68, CD163 and c-maf; mIHC for cytoxic T cells on 24 BL samples (validation cohort 2) stained for PD-1, CD8 and Granzyme B.

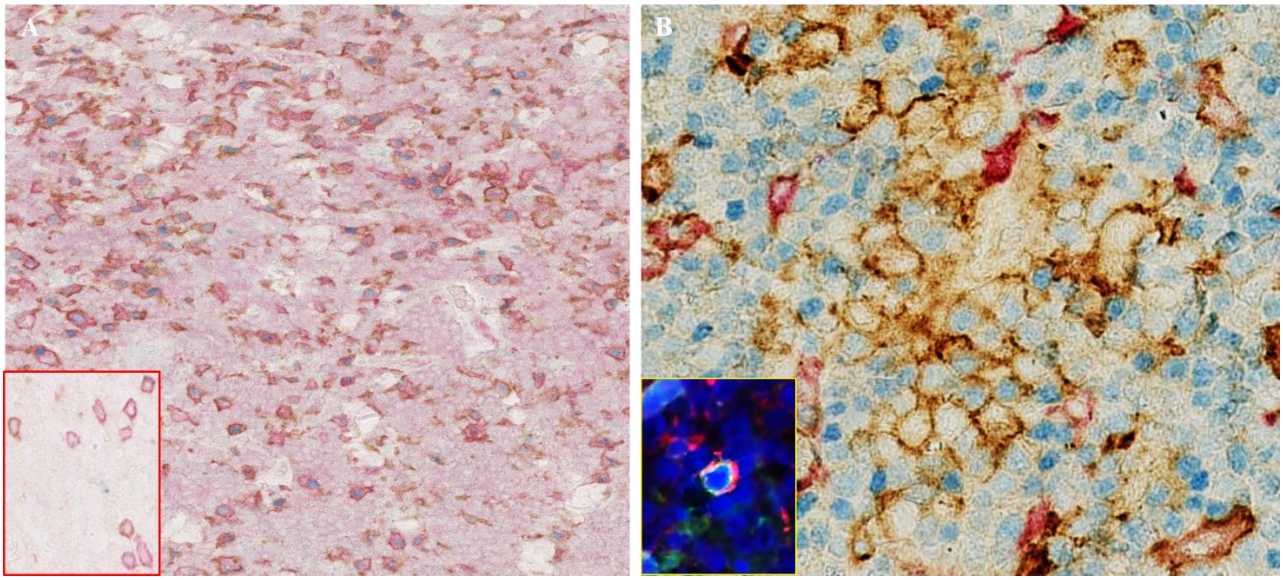

Figure 4. M2 macrophage polarization and PD-L1 expression on TAMs : A CD163 (red), c-maf (blue), PD-L1 (brown). Example of TAMs expressed M2 phenotype markers (CD163+, c-maf+) and PD-L1 in one case. (O.M: 10x). Inset: CD8 (red), Granzyme B (blue) and PD-1(brown). Pattern of PD-1 expression on cytotoxic T cells. **B** C-Myc/PD-L1/CD163 triple staining disclosed clusters of C-MYC/PD-L1 double positive cells in 4 cases characterized by co-expression of LMP2A (Inset).

Correlation between PD-L1 and LMP2A.

Preprints (www.preprints.org) | NOT PEER-REVIEWED | Posted: 18 January 2020 doi:10.20944/preprints202001.0195.v1

Since it is well known that EBV-encoded LMP1 and LMP2A can cooperate with cellular signalling pathways (i.e. Jak/Stat, IFN-γ) to regulate PD-L1 expression[30-31], we aimed to investigate whether this hold true also for those cases expressing LMP1/LMP2. We first performed Myc/PD-L1/CD163 triple staining to demonstrate the PDL1 expression on the neoplastic cells. Indeed, C-Myc/PD-L1/CD163 triple staining disclosed clusters of C-MYC/PD-L1 double positive cells in 4 cases characterized by expression of LMP2A (Table 3). PD-L1 positivity was focal and showed a heterogeneous intensity from weak to strong in 10-30% of the total tumor cells (Figure 4). The co-expression of PD-L1 and LMP2A in scattered neoplastic cells was then confirmed by double IF, identifying a possible correlation between EBV and, in particular, LMP2A in PD-L1 induction (inset Figure 4B). Of note, EBV negative BL (6 out of 40 cases) and conventional BL cases with canonical EBV type I latency characterized by the sole expression of EBNA1 (27 out of 40 cases) showed low or absent PD-L1 positivity ranging from 0% to 10% of total tumor cells. These findings indicate that PD-L1 checkpoint activation is more likely related to an unusual latency program of EBV rather than to the EBV presence itself.

DISCUSSION

Although multiple studies have investigated at tumor microenvironment (TME) and PD-L1 expression in B-cell lymphomas, only limited, small studies have been conducted in Burkitt lymphoma (BL) [14-16].

In the present study, we extensively evaluated the TME composition, activation status and expression of inhibitory immune checkpoints both on the inflammatory infiltrate and neoplastic cells of BL tumors including sporadic, endemic and HIV- associated cases. Thus, we investigated PD-L1 expression and, in addition, the possible contribution of EBV in fostering the activation of the PD1-PD-L1 axis.

The microenvironment's influence on cell proliferation and destruction varies greatly according to the inherent histotype of the lymphoma cell type [34-36]. In particular, Hodgkin lymphoma (HL) tissue often consists of relatively few monoclonal cancer cells but at least 90% non- malignant cells (e.g., regulatory T-cells), contributing to a rather unique surrounding immune ecosystem. On the other hand, BL seems to be largely devoid of such a supportive cellular environment, although the high content of TAMs might play a distinct, specific, important role in neoplastic progression through secretion of chemokines, cytokines and immune checkpoint-associated proteins as programmed- death- ligand 1 (PD-L1) [12,13].

Preprints (www.preprints.org) | NOT PEER-REVIEWED | Posted: 18 January 2020 doi:10.20944/preprints202001.0195.v1

In the recent decade a model has been developed to describe the complex mechanism of macrophage activation as a polarization towards two opposite states, namely M1 and M2, with pro- inflammatory and pro- tumoral properties respectively [37-41].

M2 macrophages are able to suppress the adaptive immune response through mechanisms including inhibition of T cell proliferation. Part of their immunosuppressive activity is exerted by their release of chemokines (CCL17, CCL18 and CCL22) that preferentially attract T cell subsets devoid of cytotoxic function. In most studies, TAM density is associated with poor prognosis[42] and the presence of M2 TAMs has been shown to correlate with poor prognosis in DLBCL[43].

In the present work, we identified a polarization towards a M2 phenotype of TAMs in all cases by applying 3 different approaches (CIBERSORT, mIF, and mIHC) regardless of the subtype of BL and thus of EBV status.

These cells, intimately associated with the neoplastic cells, constituted also the major source of PD-L1, which may inhibit the overall inflammatory response and allow the neoplastic cells to evade antitumor immunity. However, the lower rate of PD-L1 expression on TAMs in sBL may suggest a role of EBV in inducing PD-L1 expression.

PD-L1 is a major regulator of T cell function that, after engaging PD-1, leads to an altered functional state of PD-1^+ T cell exhaustion [44]. In this regard, we found that the vast majority of the CD8+ infiltrating T cells expressed PD-1 in the eBL and idBL which are frequently associated with EBV, suggesting that an adaptive immune resistance- type mechanism is active in addition to the notorious defects in HLA class II antigen presentation characterizing BL cells.

However, the role of PD-1 expression in Tumor Infiltrating Lymphocytes (TILs) on both lymphoid and epithelial malignancies is controversial. PD-1 expression in $CD8^+$ cells has been associated with the selective suppression of cytotoxic lymphocytes in nasopharyngeal carcinoma (NPC) [45]. On the other hand, the PD-1^+ TILs have also been described to lack Tim-3 expression in viral- related human papilloma virus positive (HNSCC), and thus possibly representing activated T-cells[46]. Thus, higher PD-1 detection in activated T-cells might represent a reactivation of a previous immune response in which PD-1/PD-L1 blockade occurred[35]. This is in keeping with the fact that higher PD-1 detection in activated T-cells might be a reaction to viral antigens and possibly representing a feature of virus associated tumors.

Emerging evidence in EBV- related malignancies indicates that the virus possesses the ability to actively shape the tumor microenvironment favoring its escape from anti-tumor immune responses through a variety of complex mechanisms [18]. EBV may induce a strong up- regulation of PD-L1

 doi:10.20944/preprints202001.0195.v1

expression both directly on the surface of human primary monocytes or, indirectly, on neoplastic cells, through its viral proteins LMP-1 and LMP-2 that interfere with downstream cellular signaling (i.e. AP1; JAK/STAT) [31,32] in creating an immune tolerant niche for EBV- related tumors[47-49].

Although PD-L1 expression has been largely investigated in B cell lymphomas, its expression in cellular microenviroment and in tumour cells has not been well defined in most studies[1-4].

In conclusion, our findings suggest that EBV in BL might induce PD-L1 expression on tumor cells in a minority of cases characterized by a non-canonical latency with LMP2A positivity, whereas it might influence PD-L1 upregulation on TAMs also in cases with canonical EBV type I latency. However, the prevalence of M2 macrophages as primary constituent of the TME in BL is a constant finding in all BL subtypes and thus, macrophage polarization towards a protumoral state seems an event related to the intrinsic characteristics of the tumor.

In conclusion, even if the present paper is still limited by the small sample size, our findings may shed new light on BL TME and the underlying potential mechanism of immune evasion and the cross-talk between different actors including TAMs, PD-1/PD-L1, T-cells and viral antigens which result in failure of the innate immunity in BL represented by M2 polarization. Although BL prognosis and response to conventional therapy is generally good, these data may provide a rationale for new immunotherapeutic strategies.

REFERECENS

1. Mulders, T.A; Björn, E.W. Targeting the Immune Microenvironment in Lymphomas of B-Cell Origin: From Biology to Clinical Application. *Cancers* (Basel) **2019**, *11*, 915.
2. Scott, D.W.; Gascoyne, R.D. The tumour microenvironment in B cell lymphomas. *Nat* **2014**, *14*, 517-534.
3. Xu, B.; Wang, T. Intimate cross-talk between cancer cells and the tumor microenvironment of B-cell lymphomas: The key role of exosomes. *Tumor Biology* **2017**, *39*.
4. Guna, S.Y; Ling Lee, S.W. Targeting immune cells for cancer therapy. *Redox Biol*. **2019**, *25*, 101174.
5. Ribrag, V.; Koscielny, S. Rituximab and dose-dense chemotherapy for adults with Burkitt's lymphoma: a randomised, controlled, open-label, phase 3 trial. *Lancet* **2016**, *387*, 2402-11.
6. Ngoma, T; Adde, M. Treatment of Burkitt lymphoma in equatorial Africa using a simple three-drug combination followed by a salvage regimen for patients with persistent or recurrent disease. *Br J Haematol* **2012**, *158*, 749–762.
7. God, J.M.; Haque, A. Immune Evasion by B-cell Lymphoma. *J Clin Cell Immunol*. **2013**, *5*.
8. Gopal, S.; Gross, T.G. How I treat Burkitt lymphoma in children, adolescents, and young adults in sub-Saharan Africa. *Blood* **2018**, *132*, 254-263.
9. Bouda, G.C.; Traorè F. Advanced Burkitt Lymphoma in Sub-Saharan Africa Pediatric Units: Results of the Third Prospective Multicenter Study of the Groupe Franco-Africain d'Oncologie Pediatrique. *J Glob Oncol*. **2019**, *5*, 1-9.
10. Silva, W.F.D.; Garibaldi, P.M.M. Outcomes of HIV-associated Burkitt Lymphoma in Brazil: High treatment toxicity and refractoriness rates - A multicenter cohort study. *Leuk Res*. **2019**, *10*:106287.
11. Ford, C.A.; Petrova, S. Oncogenic Properties of Apoptotic Tumor Cells in Aggressive B Cell Lymphoma. *Curr Biol* **2015**, *25*, 577-588.
12. Pham, L.V.; Pogue, E. The Role of Macrophage/B-Cell Interactions in the Pathophysiology of B-Cell Lymphomas. *Front Oncol*. **2018**, *8*, 147.
13. Kumar, D.; Xu, M. L. Microenvironment Cell Contribution to Lymphoma Immunity. *Front Oncol*. **2018**, *8*, 288.
14. Majzner, R.G.; Simon, J.S. Assessment of programmed death-ligand 1 expression and tumor-associated immune cells in pediatric cancer tissues. *Cancer* **2017**, *123*, 3807-3815.
15. Chen, B.J.; Chapuy, B. PD-L1 Expression Is Characteristic of a Subset of Aggressive B-cell Lymphomas and Virus-Associated Malignancies. *Human Cancer Biology* **2013**, *19*, 3462-3473.
16. Tan, G.W.; Visser, L. The Microenvironment in Epstein–Barr Virus-Associated Malignancies. *Pathogens* **2018**, *7*, 40.
17. Rowe, M.; Fitzsimmons, L. Epstein-Barr virus and Burkitt lymphoma. *Chin J Cancer* **2014**, *33*, 609-619.
18. Dolcetti, R. Cross-talk between Epstein-Barr virus and microenvironment in the pathogenesis of lymphomas. *Semin Cancer Biol*. **2015**, *34*, 58-69.
19. Dojcinov, S.D.; Fend, F. EBV-Positive Lymphoproliferations of B- T- and NK-Cell Derivation in Non-Immunocompromised Hosts. *Pathogens*. **2018**, *7*, 28.

20. Linke-Serinsöz E; Fend, F; Quintanilla-Martinez, L. Human immunodeficiency virus (HIV) and Epstein-Barr virus (EBV) related lymphomas, pathology view point. *Semin Diagn Pathol*. **2017**, *34*, 352-363.
21. Anastasiadou, E.; Stroopinsk, D. Epstein−Barr virus-encoded EBNA2 alters immune checkpoint PD-L1 expression by downregulating miR-34a in B-cell lymphomas. *Leukemia* **2019**, *33*, 132-147.
22. Vargas-Ayala, R.C.; Jay, A. Interplay between the epigenetic enzyme lysine (K)-specific demethylase 2B and Epstein-Barr virus infection. *J. Virol* **2019**, *14*, 13.
23. Granai, M.; Ambrosio, M.R. Role of Epstein Barr Virus In Transformation Of Follicular Lymphoma To Diffuse Large B-Cell Lymphoma: A Case Report And Review Of The Literature. *Haematol* **2019**, *104*.
24. Rivera-Soto, R.; Damania B. Modulation of Angiogenic Processes by the Human Gammaherpesviruses, Epstein–Barr Virus and Kaposi's Sarcoma-Associated Herpesvirus. *Front Microbiol* **2019**, *10*, 1544.
25. Chen, B.; Khodadoust, M. S. Profiling tumor infiltrating immune cells with CIBERSORT. *Methods Mol Biol*. **2018**, *1711*, 243-259.
26. Piccaluga, P.P.; De Falco, G. Gene expression analysis uncovers similarity and differences among Burkitt lymphoma subtypes. *Blood* **2011**, *117*, 3596–3608.
27. Abate, F.; Ambrosio, M.R. Distinct Viral and Mutational Spectrum of Endemic Burkitt Lymphoma. *PLoS Pathog* **2015**, *11*.
28. Parra, E.R.; Uraoka, N. Validation of multiplex immunofluorescence panels using multispectral microscopy for immune-profiling of formalin-fixed and paraffin-embedded human tumor tissues. *Sci. Rep*. **2017**, *7*.
29. Swerdlow, S.H.; Campo, E. *WHO Classification of Tumours of Haematopoietic and Lymphoid Tissues*, 4th Edition; IARC: Lyon, France, 2008.
30. Marafioti, T.; Paterson, J.C. The inducible T-cell co-stimulator molecule is expressed on subsets of T cells and is a new marker of lymphomas of T follicular helper cell-derivation. *Haematol* **2010**, *95*, 432-439.
31. Bi, X.; Wang, H. PD-L1 is upregulated by EBV- driven LMP1 through NF-kB pathway and correlates with poor prognosis in natural killer /T-cell. *J HEMATOL ONCOL* **2016**, *9*.
32. Hudnall, S.D.; Küppers, R. *Precision Molecular Pathology of Hodgkin Lymphoma*, 1st Edition; Springer: 2018.
33. Fowler, N.H.; Cheah, C. Y. Role of the tumor microenvironment in mature B-cell lymphoid malignancies. *Haematol* **2016**, *101*, 531-540.
34. Shain, K.H.; Dalton, W.S. The tumor microenvironment shapes hallmarks of mature B-cell malignancies. *Oncogene* **2015**, *34*, 4673-82.
35. Wang, M.; Zhao, J. Role of tumor microenvironment in tumorigenesis. *J Cancer* **2017**, *8*, 761-773.
36. Zen Petisco Fiore, A.P; de Freitas Ribeiro, P. Sleeping Beauty and the Microenvironment Enchantment: Microenvironmental Regulation of the Proliferation-Quiescence Decision in Normal Tissues and in Cancer Development. *Front. Cell Dev. Biol*. **2018**.
37. Xue, J.; Schmidt, S.V. Transcriptome-Based Network Analysis Reveals a Spectrum Model of Human Macrophage Activation. *Immunity* **2014**, *40*, 274-288.
38. Steidl, C.; Lee, T. Tumor-Associated Macrophages and Survival in Classic Hodgkin's Lymphoma. *N Engl J Med*. **2010**, *362*, 875-885.

39. Li, Y.L.; Shi, Z.H. Tumor-associated macrophages predict prognosis in diffuse large B-cell lymphoma and correlation with peripheral absolute monocyte count. *BMC Cancer* **2019**, *19*,1049.
40. Larionova, I.; Cherdyntseva, N. Interaction of tumor-associated macrophages and cancer chemotherapy. *Oncoimmunology* **2019**, *8*, 1596004.
41. Komohara, Y.; Niino, D. Clinical significance of CD163+ tumor-associated macrophages in patients with adult T-cell leukemia/lymphoma. *Cancer Sci* **2013**, *104*, 945–951.
42. Bingle, L.; Brown, N.J. The role of tumour associated macrophages in tumour progression: implications for new anticancer therapies. *J Pathol* **2002**, *196*, 254–265.
43. Nam, S.J.; Go, H. An increase of M2 macrophages predicts poor prognosis in patients with diffuse large B-cell lymphoma treated with rituximab, cyclophosphamide, doxorubicin, vincristine and prednisone. *Leuk Lymphoma* **2014**, *55*, 2466–2476.
44. Jiang Y.; Li Y. T-cell exhaustion in the tumour microenviroment. *Cell Death Dis* **2015**, *6.*
45. Larbcharoensub, N.; Mahaprom, K. Characterization of PD-L1 and PD-1 Expression and CD8+ Tumor-infiltrating Lymphocyte in Epstein-Barr Virus-associated Nasopharyngeal Carcinoma. *Am J Clin Oncol* **2018**, *41*, 1204-1210.
46. Shayan, G.; Ferris, R.L. PD-1 blockade upregulate TIM-3 expression as a compensatory regulation of immune check point receptors in HNSCC TIL. *J Immunother Cancer* **2015**, *3*, 196.
47. Wasil, L.R.; Tomaszewski, M.J. The effect of Epstein-Barr virus Latent Membrane Protein 2 expression on the kinetics of early B cell infection. *PLoS One* **2013**, *8*.
48. Deb Pal, A.; Banerjee, S. Epstein–Barr virus latent membrane protein 2A mediated activation of Sonic Hedgehog pathway induces HLA class Ia downregulation in gastric cancer cells. *Virology* **2015**, *484*, 22-32.
49. Rancan, C.; Schirrmann, L. Latent Membrane Protein LMP2A Impairs Recognition of EBV-Infected Cells by CD8+ T Cells. *PLoS Pathog* **2015**, *11*.